Novel full-ceramic monoblock acetabular cup with a bioactive trabecular coating: design, fabrication and characterization

Francesco Baino[a,*], Joaquim Minguella[b], Nicholas Kirk[c], Maria Angeles Montealegre[d], Cosima Fiaschi[e], Feza Korkusuz[f], Gissur Orlygsson[g], Chiara Vitale-Brovarone[a]

[a]*Institute of Materials Physics and Engineering, Applied Science and Technology Department, Politecnico di Torino, Corso Duca degli Abruzzi 24, 10129 Torino, Italy*

[b]*Fundació Centre CIM (UPC-BarcelonaTECH), C/ Llorens i Artigas 12, 08028 Barcelona, Spain*

[c]*Glass Technology Services (GTS) Ltd, 9 Churchill Way, Sheffield S35 2PY, United Kingdom*

[d] *AIMEN Technology Centre, Relva 27A – Torneiros, 36410 Porriño, Pontevedra, Spain*

[e] *EXEMPLAR, Corso Vittorio Emanuele II 161, 10139 Torino, Italy*

[f]*FAME-MED Medical Ltd, Hacettepe University Technocity, 06800 Ankara, Turkey*

[g] *Innovation Center Iceland (ICI), Arleynir 2-8, 112 Reykjavik, Iceland*

* Corresponding author: F. Baino

Tel.: +39 011 090 4668

Fax: +39 011 090 4624

E-mail: francesco.baino@polito.it

Abstract

Over the last 25 years, the philosophy behind an optimal fixation of orthopaedic implants to hard tissues progressively evolved towards "bone-conservative" solutions in order to minimize bone resection/loss and maximize tissue-implant integration. Hence, the researchers' attention moved from "traditional" fixation of the prosthesis to host bone by using screws or acrylic cement to new strategies based on physico-chemical bonding and surface modification of the implant. This research work explores the feasibility of a novel bioceramic monoblock acetabular cup for hip joint prosthesis that can be fixed to the patient's bone by means of a bone-like trabecular coating able to promote implant osteointegration. Sponge replica method was properly adapted and optimized to produce hemispherical foam-like bioactive glass-ceramic coatings that were joined to Al_2O_3/ZrO_2 composite cups by the interposition of a glass-ceramic interlayer. Morphological analyses by scanning electron microscopy (SEM) and micro-computed tomography revealed the good quality of joining at the different interfaces. Preliminary investigation of the mechanical properties was carried out to evaluate the suitability of the device for biomedical use. *In vitro* bioactive behaviour was assessed by immersion studies in simulated body fluid and evaluating the apatite formation on the struts of the trabecular coating. The concepts and findings reported in the present work can have a significant impact in the field of implantable devices, suggesting a valuable alternative to currently-applied but often suboptimal techniques for bone-prosthesis fixation.

Keywords: Bioceramics; Coating; Bioactive glass; Glass-ceramic; Scaffold; Hip joint prosthesis.

1. Introduction

The hip prosthesis has been an active area of joint replacement research and development for more than one hundred years. The earliest recorded attempts at hip replacement, which date back to 1890 and were carried out in Germany, used an ivory sphere to replace the femoral head [1]. Fifty years later, Moore reported and performed the first metallic hip replacement surgery using the Co-Cr alloy called Vitallium [2]. A major breakthrough in hip replacement surgery, which resulted in decreased loosening, was achieved by Charnley who from 1962 onwards used acrylic bone cement to fix the prosthetic components to host bone [3]. Since then, Charnley's design has been considered very successful and the use of cement is now the most widely adopted strategy for prosthesis fixation worldwide.

Over time, however, the cement ages and disintegrates postoperatively thereby producing debris, which may ensue in the so-called "cement disease" yielding implant mobilization and osteonecrosis at the operation site [4]. Therefore, from the 1970s onwards a number of other prostheses were developed with the primary aim of eliminating the need for bone cement [5-7]. Press-fit prostheses were designed to fix in place by close fit alone. Threaded metal acetabular components which were intended to be screwed into bone were also developed. The surface of metal prostheses was also locally treated so that the parts of the implant adjacent to bone had small beads or meshes: the aim was to encourage bone ingrowth into the pores of the prosthesis surface to produce firm fixation. Porous acetabular metal backs may loosen by particle release, inflammation, metal hypersensitivity and oxidative stress. Tissue ingrowth into porous titanium acetabular metal backs is as low as 12% [8].

Modifying the surface properties by the deposition of a coating is a further approach to avoid the use of cement and improve osteointegration while maintaining good mechanical properties of the prosthesis [9]. Hydroxyapatite (HA)-coated metal femoral stems have been proposed as an effective alternative to cemented implants, especially for young and active patients. In this regard, most

clinical trials have focused on the performance of the femoral component and demonstrated the benefits of the HA-coated implants with respect to the untreated ones; more controversial results have been reported in the case of the acetabular component, also due to the relative paucity of relevant studies. HA-coated threaded hemispherical acetabular cups demonstrated improved fixation radiographically at a minimum of 3 years compared to threaded metal acetabular cups without a HA coating [10,11]. Moilanen et al. [12] reported the long-term results (3 postoperative years) for press-fit Co-Cr acetabular components with a central peg and two superolateral flanges with or without a 80 to 120 μm thick HA coating: from a clinical viewpoint, no significant differences between the two implants were observed, but the HA-coated cups were generally associated with less rotational and proximal migration. As underlined by Jaffe and Scott in an interesting review [9], HA-coated metal acetabular cups have proved to be equal to non-coated components with regard to the achievement of a prompt biological fixation.

Since the 1980s, both acetabular and femoral components have been made modular by many manufacturers. This model style involves housing an acetabular liner in a metal shell (the so-called metal-back) that can be anchored to the patient's bone with or without acrylic cement. However, issues associated to traumatic fixation with significant bone resection and wear of the ultra-high molecular weight polyethylene (UHMWPE) acetabular cup still linger on. In recent years, use of highly-crosslinked UHMWPE has yielded promising results to diminish the risks associated to polymer wear [13,14]. Another trend is the elimination of UHMWPE from orthopaedic components by using bearing couples consisting of metal-on-metal (e.g., Co-Cr–on–Co-Cr) or ceramic-on-ceramic (e.g. alumina-on-alumina) [15].

Ceramic surfaces offer a major benefit of drastically reduced wear rates and excellent long-term biocompatibility which can increase the longevity of prosthetic hip joints [16]. This benefit is important clinically since hip replacement is now a common surgical procedure that is increasingly performed on younger patients who place greater demands on the prosthetic bearings. However, as the presence of the metal-back in the modular design reduces the volume available for the

acetabular liner, the use of ceramics can become a problem particularly for bearing couples with large femoral heads [17]. This issue was recently pointed out by Solarino et al. as one of the most challenging research topics in modern orthopaedic surgery [18]. As underlined by Schreiner et al. [19], a stable osteointegration of an alumina or alumina-matrix composite ceramic could facilitate the use of a thin-walled monoblock acetabular cup for hip arthroplasty with large femoral heads providing advantages like reduced risk of implant dislocation. In this regard, porous-surfaced ceramic implants have been recently experimented, reinterpreting the idea behind the development of surface-textured metal prostheses introduced more than 30 years ago. Compared to untreated implants, alumina/zirconia composites with a porous surface exhibited better osteointegration upon implantation in young pigs (12 weeks) [19] and sheep (52 weeks) [20].

This work has moved an important step forward. Our research group first claimed the concept that a full-ceramic monoblock acetabular cup for hip joint prosthesis could be anchored to the patient's bone without employing a metal-back, screws or acrylic cement (thus avoiding the risks and limitations associated to implant modularity and malposition, traumatic fixation, toxicity due to metal ion release and/or cement degradation) by means of a bioactive trabecular coating. This innovative concept has been disclosed in a patent [21] and further developed in the framework of the EC-funded project MATCh ("Monoblock acetabular cup with trabecular-like coating"). As schematically illustrated in Fig. 1, this novel prosthetic acetabular cup is constituted by three layers, i.e. an alumina/zirconia composite substrate, a bioactive glass-based trabecular coating and a glass-derived interlayer with the aim of improving the adhesion between the bioceramic cup and the trabecular coating. The key element of this 3-layer system is the outer bone-like coating, as new bone is expected to grow *in vivo* within its network of interconnected macropores creating a tight interfacial bond. Many experimental studies have demonstrated that bioactive glasses and glass-ceramics can form a strong bond with bone tissue upon implantation *in vivo* and, particularly if processed in a porous form (3-D scaffold), can stimulate osteogenesis at the implant site [22-25]; for the first time, our research group has proposed the use of a bioactive glass-derived scaffold as

the key osteointegrative element of a complex prosthetic device (Fig. 1). Previous studies demonstrated the feasibility of this device in a flat geometry [26,27] and in a simplified curved configuration [28-30]; the challenge presented in this work is to develop a processing schedule to produce a real, complete prototype such as the one depicted schematically in Fig. 1, which also was the main objective of the EC-funded project MATCh.

2. Materials and methods

2.1. Starting materials

Alumina-matrix bioceramic cups were fabricated in-house by subtractive methodology followed by sintering, according to a processing schedule described elsewhere [31]. The composition of the cups ($75Al_2O_3$-$25ZrO_2$ wt.%) was similar to that of Biolox delta (CeramTec, Germany), that is commonly recognized as the "gold standard" material to fabricate ceramic liners for hip prosthesis. Small-size (nominal outer diameter 28.0 mm, diameter of the niche 15.5 mm) and large-size cups (nominal outer diameter 39.0 mm, diameter of the niche 27.0 mm) were produced to mimic two of the standard types available on the market.

Two glass compositions were adopted to manufacture the dense coating (S57A7, $57SiO_2$-$30CaO$-$6Na_2O$-$7Al_2O_3$ mol.%) and the trabecular layer (S50B2, $50SiO_2$-$35CaO$-$7Na_2O$-$6P_2O_5$-$2B_2O_3$ mol.%), respectively. Criteria of design and selection as well as the characterization of these glasses are reported elsewhere [32]. S57A7 and S50B2 were individually manufactured and the mixed high-purity raw materials (oxides and carbonates) added to platinum crucibles for subsequent melting. Melting was carried out in an electrically heated furnace and melts were all made at 1450 °C, which was assessed to be sufficient to allow melting and homogenisation. The individual melts of glass were cast as single solid blocks and then thermally shocked in de-ionized water to produce

the precursor materials for the further crushing and grinding. Glass powders were eventually sieved by using stainless steel sieves to obtain particles with size below 32 μm.

2.2. Fabrication of the dense coating (interlayer)

A layer of S57A7 was applied on the outer surface of the bioceramic cup by dip-coating technique. A 3-component slurry was prepared by mixing S57A7 powder, poly(vinyl alcohol) (PVA) and distilled water (40 : 6 : 54 wt.%). PVA acted as a binder in order to promote the adhesion of glass particles to the curved surface of the ceramic cup. After PVA dissolution under continuous magnetic stirring (200 rpm) at around 90 °C, glass powder was added to the batch. The water evaporated during PVA dissolution was also re-added to maintain the original weight ratio among the constituents (we weighed the beaker containing the slurry immediately after preparation and, then, after PVA dissolution: the mass difference corresponds to the amount of water evaporated). Homogeneity of the slurry was ensured by further stirring for 30 min at room temperature.

A key technological challenge in the manufacturing of the coating was the development of a simple and effective strategy to manipulate the bioceramic cup upon the dip-coating process. For this purpose, a sample-holder system was designed that comprised a plastic tube hosting a peg which can slide through the central tunnel (Fig. 2). This device allowed the operator to safely manipulate the bioceramic cup without any direct contact with (and possible damage to) the deposited glass coating.

The cup was attached to the sample-holder by bi-adhesive tape, then a controlled dipping process into the S57A7 slurry was carried out to ensure that the external surface was completely submerged by the suspension (Figs. 2a and b); special care was required to avoid liquid percolation in the hemispherical niche intended to articulate with the femur head. After static soaking for 2 s, the cup was taken back from the beaker and manually rotated to avoid local accumulation of the slurry due to gravity, so that a coating with uniform thickness could be obtained (Fig. 2c). The rotation

continued for 30 min till the coating was dry. Afterwards, the dip-coating cycle was iterated to increase the thickness of the glass layer on the bioceramic cup (about 50 μm), whilst the slurry was continuously mixed in the beaker to avoid the sedimentation of glass particles. At the end of the process, the glass-coated cup was removed from the sample-holder by pushing the plastic peg (Fig. 2d), left to dry for 6 h under ambient conditions and thermally treated in an electrically-heated furnace at 1000 °C for 1 h (heating rate 5 °C min^{-1}).

2.3. Fabrication of the trabecular coating

Sponge replication allows the fabrication of porous ceramic products by using a polymeric sponge as a sacrificial template that is soaked in the slurry, squeezed to remove the excess suspension from the pores and eventually burnt-out to obtain an inorganic replica of the 3-D foam structure [33]. This technique is generally recognized as a highly effective and versatile method to process bioactive glasses in the form of bone-like porous scaffolds [32], and early results attained in previous studies by our research team demonstrated the suitability of this method to fabricate trabecular coatings on flat prosthetic implants [26,27]. In order to effectively apply the trabecular coating to a "real" bioceramic cup that is to be used in hip joint surgery, there were two key questions to answer: (i) how to impart a shell-like shape to the porous polymeric template?, and (ii) how to remove the excess slurry from the pores of the polymeric foam in this particular configuration?

In order to find an appropriate answer to these questions, the research team designed and developed an original series of *ad-hoc* tools for manipulating and processing the open-cell polyurethane (PU) sponge (apparent density 20 kg m^{-3}) used as a template. First, a special metal mould was fabricated and successfully tested to impart a hemispherical shell-like shape to the foam (Fig. 3). The mould is made by two aluminium plates; the upper plate can slide along two stainless steel columns inserted firmly in the lower plate (Fig. 3a). The central hole hosts the Al_2O_3/ZrO_2 composite cup, the profile

of which is perfectly followed by the PU sponge that is held in position by the upper plate. From an operative viewpoint, the empty mould is introduced into a furnace at room temperature and then heated up to 140 °C; after 1 h, the PU sponge (10 cm × 10 cm square piece, thickness 5 mm) is introduced into the mould that can be then closed and heated to 140 °C for 12 h. The mould is left to cool, then extracted from the furnace and opened to allow the removal of the shaped sponge (Figs 3b and c). The excess sponge is cut away by a knife. Fig. 3c shows that the shaped sponge maintains a uniform thickness along its profile. Two metal moulds were designed and developed to process samples of different sizes (small and large bioceramic cups, see the section 2.1).

The shell-shaped sponge was then attached to the bioceramic cup by a thin film of glue (which will be thermally removed upon sintering) to temporarily bond the two components together and allow safe manipulation. This approach permitted manipulation (without unwanted compressions) of the shell-shaped sponge which would have been very difficult, unless supported – the most appropriate support was the cup itself to which the sponge was attached.

The sample-holder described in the section 2.2 and shown in Fig. 2 was also used to manipulate the cup with the attached shell-shaped sponge during the sponge impregnation/compression procedures in order to avoid the risk of accidental and unwanted squeezing. The sample was soaked for 1 min into a 3-component slurry prepared by mixing S50B2 powder, PVA and distilled water (40 : 6 : 54 wt.%; the details of slurry preparation are analogous to those reported in the sect. 2.2) so that the suspension could infiltrate the pore space; afterwards, the sample was taken back and placed in the squeezing system to achieve the desired slurry saturation.

The development of a reliable system for the compression of the slurry-impregnated shell-shaped sponge was a crucial and challenging aspect of this work. The adopted solution involves the use of a squeezing system constituted by a supporting hollow cylinder, a plastic square plate with a central hole hosting the sample to be squeezed and 2 pierced hemispherical hemi-shells (here, the term “shell” denotes a complete hemisphere) the function of which is to compress the slurry-impregnated sponge (Fig. 4). The two pierced hemi-shells are connected to the square base by 4 pins acting as

sliding guides. The squeezing system was designed to be used in combination with the sample-holder of the cup (Figs. 5a and b). This innovative solution allowed the possible risks associated with the sample manipulation to be controlled throughout the whole sponge replication process, as the sample is fixed to the sample-holder and the slurry-impregnated sponge is not manually handled. Sponges with flat surfaces (e.g. cubes [35,36] or strips [26,28]) can be effectively and uniformly compressed by means of an axial press; however, the situation is much more complex in the case of curved samples since, ideally, a compression along the radial direction should be performed. A simplified strategy was adopted in this work and the principle behind the action of the two hemi-shells is schematically depicted in Fig. 4. Briefly, instead of performing the compression along the radial direction – which would have required a high technological investment –, the pressing action was split in two components along the x and y directions on the vertical plane (Fig. 4). In such a way, a quite uniform compression of the sponge on the vertical plane can be achieved. First the compression downward (along the y axis) was performed and then a second compressive action was exerted putting in contact the 2 hemi-shells (compression along the direction x). The two hemi-shells can slide along 2 pins and 2 small guides. The height of the pins and the initial half distance between the hemi-shells are equal to δ (2 mm), which corresponds to the desired reduction in thickness of the sponge (Fig. 4).

As illustrated in Fig. 4 (top), the compression on the horizontal plane is maximum in the points A and B and minimum in the points C and D; therefore, after a first compression the sample was rotated 90° to achieve a homogeneous squeezing action along the whole sponge profile. This double-compression cycle (at 0 and 90°) is iterated for 3 times; then, the sample is extracted from the squeezing device and, after 1 min, soaked again into the slurry. After three cycles of sponge impregnation/compression, an additional cycle of impregnation without any subsequent compression was performed.

Part of the process is illustrated in Figs. 5a and b. Two squeezing devices were designed and developed to be applied to bioceramic cups of different size (Fig. 5b). The samples were left to dry

first under ambient conditions for 3 h and then at 70 °C for 3 h; the resulting "greens" are shown in Figs. 5c and d. A heat treatment at 1000 °C for 3 h in an electrically heated furnace (heating rate 5 °C min^{-1}) allowed removing all organic matter, sintering the S50B2 particles (formation of the trabecular coating) and joining the porous layer to the dense S57A7 coating lying underneath.

2.4. Characterisation

Full characterization of S57A7 and S50B2 glasses, including the glass-ceramic products obtained from them after sintering, has been reported elsewhere [32].

The morphology of the samples prepared in the present work was investigated by scanning electron microscopy (SEM, FEI QUANTA INSPECT). Samples were metal-coated prior to the analysis and observed at an accelerating voltage of 15 kV. Selected samples were also embedded in epoxy resin (Epofix, Struers), cut and polished using #600 to #4000 SiC grit paper for SEM analysis of the cross-section. Compositional analysis was performed by energy dispersive spectroscopy (EDS; Philips EDAX 9100). Gradual changes in chemistry across the S57A7 interlayer/bioceramic substrate were visualised using EDS elemental line profiles.

The samples were non-destructively investigated by X-ray micro-computed tomography (micro-CT; General Electric, Phoenix). The source voltages and currents were 130 kV and 150 μA for the analysis of the S57A7 coating, with a voxel size of 5.1 μm, and 130 kV and 90 μA for the analysis of the S50B2-derived trabecular layer, with a voxel size of 8.6 μm. Reconstruction was performed with Datos-x reconstruction software accompanying the scanner, and visual evaluation and detail measurements were done by VGStudioMax 2.0 from Volume Graphics.

The adhesion strength of S57A7 coatings was assessed following the ASTM standard [37]. Small bioceramic disks (diameter 8.6 mm, height 2 mm), produced under the same conditions adopted for the cups, were used as substrates suitable for the mechanical tests. S57A7-coated samples were firmly attached to two loading fixtures (16-mm diameter steel cylinders to be connected to the

testing machine by metal pins) using an epoxy resin (Araldite® AV 119, Ciba-Geigy), which is able to withstand a maximum tensile stress of about 40 MPa (as declared by the manufacturer). At room temperature the adhesive was a gel and its polymerization was achieved by a low-temperature treatment in an oven at 140 °C for 1 h. Maintaining the coaxiality of the fixtures is a crucial issue to obtain reliable results; therefore, an *ad-hoc* tool was developed with circular guides matching the fixtures size and allowing coaxiality upon resin hardening, in order to avoid misalignment problems. The adhesion strength of the coating was assessed by applying a tensile load to the samples (Syntech 10/D machine, MTS Corp.; cross-head speed of 1 mm min^{-1}) and calculated as L_t / A_t , wherein L_t (N) is the failure tensile load and A_t (mm^2) is the area on which the load was applied. The result was expressed as mean value ± standard deviation calculated on 10 samples.

In vitro bioactivity tests were carried out by soaking the samples in a simulated body fluid (SBF) prepared according to Kokubo's protocol [38]. The samples were incubated under static conditions at 37 °C in 30 ml of SBF contained in PE bottles. Every 48 h the samples were extracted from the bottles, gently rinsed with some drops of distilled water and then soaked in 30 ml of new SBF. Periodic replacement of SBF is a common experimental practice to simulate fluid circulation in the human body [39-42] as the cation concentration in the solution progressively decreases during the experiment as a result of changes in the sample surface chemistry. The pH of the solution was monitored daily. At the end of the experiment (7 days), the samples were left to dry under ambient conditions and then investigated by SEM and EDS.

3. Results and discussion

3.1. Dense coating (interlayer)

The appearance of S57A7-coated small cups (diameter about 28 mm) before and after sintering is compared in Figs. 6a and b, respectively. The white, shiny aspect of the heat-treated S57A7 coating

(Fig. 6b) suggests its glass-ceramic nature, in accordance to previous results reported elsewhere [32]. Small- and large-size cups (Fig. 6c) are coated by a continuous S57A7 layer; uncoated regions were not noticed by a naked eye visual inspection.

The cross-sectional SEM micrograph reported in Fig. 7a and acquired on a large portion of the sample shows that the cup is continuously and quite uniformly coated by the S57A7 layer along the cross-section. Fig. 7b qualitatively reveals an excellent adhesion between S57A7 coating and Al_2O_3/ZrO_2bioceramic substrate, without significant cracks or flaws at the interface. A moderate porosity characterized by small closed pores with size below 10 μm is probably due to the presence of gas bubbles that remained entrapped in the coating during the manufacturing process and/or are associated to the burn-off of PVA upon thermal treatment; this is in agreement with previous observations by the authors [29].

Elemental line profiles reported in Fig. 8 suggest the existence of a transition zone at the coating/substrate interface originated by atomic diffusion upon thermal treatment. The elemental profile for Si shows the typical linear trend of functionally graded materials [43]. Al^{3+} ions have migrated from the cup into the coating region near to the interface; this phenomenon was already observed by the authors analysing other biomedical glass coatings on alumina substrates [26,44]. Furthermore, there is a progressive decrease of Na abundance in the coating as the interface is approached. Therefore, a physico-chemical joining of the S57A7 coating to the substrate exists, which is expected to ensue in a good adhesion between these two elements.

Fig. 7c shows a top three-fourths view of the S57A7-coated cup; the coatings is distinguishable by some surface irregularities visible in the bottom part of the cup and, especially, on its top. A higher resolution image of the cup coated with S57A7 is shown in Fig. 7d. In this segment the coating is around 50-70 μm thick. The adhesion of the coating to the substrate is expected to be very good as no cracks can be detected both at the substrate/coating interface and in the coating itself, in good agreement with SEM observations (Figs. 7a and b).

Quantification of the bonding strength was carried out by mechanical tests on S57A7-coated small bioceramic disks; tensile tests yielded an adhesion strength of 27.4 ± 10.0 MPa. This value is comparable to that assessed by the authors in the case of SiO_2-CaO-Na_2O-Al_2O_3 coatings deposited on alumina substrates by airbrush spraying [29,45]. Referring to international standards, a tensile stress of (at least) 15 MPa is recommended for HA coatings on surgical implants [46]; therefore, the high adhesion strength obtained for the S57A7 coatings suggests their mechanical suitability for clinical use.

3.2. Trabecular coating

A typical example of complete prototype (bioceramic cup + S57A7 interlayer + S50B2 trabecular coating) is shown in Figs. 9a and b which demonstrate the high quality of the device produced (the trabecular-like layer is well-adherent to the substrate, without any discontinuity or macro-defects). As reported in a previous work [32], upon high-temperature thermal treatment S50B2 partially crystallizes, thus resulting in a glass-ceramic trabecular coating.

Fig. 9c provides a micro-tomographic reconstruction of the surface topography of the S50B2 coating in the top part of the cup, and a SEM micrograph of the trabecular 3-D architecture of the coating is shown in Fig. 9d. The open-cell highly-interconnected porous structure of the starting polymeric template was successfully replicated by the final sintered trabecular layer that coats continuously the outer surface of the cup. The struts are well-densified and the pore size is within 100-500 μm, which is in the optimal range recommended in the literature for bone tissue engineering porous grafts [47].

Results from micro-tomographic analyses of the coating are presented in Fig. 10. Along the cross-section, the thickness of the S50B2 trabecular layer ranges from 0.7 to 1.5 mm in the top region whereas it reaches up to 2.8 mm on the edges (Fig. 10a). There is a range in the thickness of the coating, the thinnest part being in the region around the top of the cup, and the thickest being near

the edges; this is probably due to the downward percolation of the slurry upon drying of the S50B2-loaded sponge. Figs. 10b-f further confirm that the S50B2 trabecular coating is completely attached to the whole outer surface of the cup, in good agreement with the top view reported in Fig. 9c, without cracks or discontinuities with the S57A7 interlayer lying underneath (Fig. 10g). Excellent adhesion was possible due to a careful design of the composition of starting glasses [32] and control of the processing parameters. Furthermore, localised melting between trabecular coating (S50B2) and interlayer (S57A7) occurred at the contact regions upon sintering, which further contributes to the creation of an intimate strong bond between the two materials. Average total porosity of the trabecular coating was estimated about 75.0 vol.%, with a very limited amount of closed pores (2.3 vol.%). The presence of an interconnected network of open pores is fundamental in the light of the intended application of the device in an *in vivo* scenario, since it is vital that there are paths for cells to migrate, tissue to grow in and waste products to flow out.

Mechanical characterization of the whole device was not performed in this research due to the complexity of this issue which would require the testing of non-standard specimens (samples with hemispherical shape) and, consequently, the development of *ad-hoc* protocols and tools. However, mechanical tests performed on S50B2 porous cuboids with 3-D strut architecture analogous to that of the hemispherical trabecular coating yielded promising results [32]: S50B2 scaffolds have a compressive strength which is superior to that of cancellous bone (2-12 MPa [48]), which supports its suitability for load-bearing prosthetic applications.

Results from *in vitro* bioactivity studies in SBF are reported in Fig. 11. The SEM back-scattered imaging mode emphasized the presence of a newly formed phase on the struts of the S50B2 trabecular coating, as shown in Figs. 11a and b. Compositional analysis by EDS (Fig. 11c) revealed that this new phase is rich in calcium (Ca) and phosphorus (P) with a Ca/P atomic ratio (about 1.2) typical of Ca-deficient nanocrystalline HA that usually nucleates *in vitro* on the surface of bioactive glasses.

The presence of an apatite-like layer on the struts of the trabecular coating is expected to play a key role *in vivo* promoting colonization by bone cells, as it was widely demonstrated that osteoblasts attach and spread preferably on nanocrystalline apatite due to its chemical and crystallographic similarity to bone mineral [22,49]. By using an evocative image, the apatite layer can be viewed as a "biomimetic skin" that makes the surface, struts and pore walls of the trabecular coating a highly biocompatible substrate for cell adhesion.

Upon soaking in SBF, the pH variations induced by ion leaching phenomena were moderate without exceeding the maximum value of 7.70 (reached after the early 48 h of immersion). This finding is in good agreement with previous observations on S50B2 cuboids soaked in SBF [32]. Therefore, no cytotoxic effect due to a sharp increment of alkalinity is forecast in an *in vivo* scenario.

There is a general consensus in the scientific community that the *in vitro* formation of an apatite-like layer on the biomaterials surface is a sort of precondition so that the implant can tightly bond to bone *in vivo*. A common drawback of metal (e.g. titanium and Co-Cr alloys) and bioinert ceramic implants (e.g. alumina, zirconia and composites thereof) is that, once implanted *in vivo*, they induce the formation of a non-adherent fibrous capsule at the tissue-implant interface, which could involve postoperative mobility and displacement of the prosthetic component from the correct position. On the contrary, not only S50B2 should form a tight bond with host bone *in vivo*, but new bone tissue is expected to grow within the interconnected porous network of the trabecular coating. This hypothesis is supported by a number of studies on the bone regenerative potential of bioactive glasses and glass-ceramics [22] and it is particularly interesting to mention the results reported by Hamadouche et al. [50], who observed greater bone tissue formation around alumina implants coated with sol-gel bioactive glass compared to bulk alumina implants (study in a rabbit model). Despite the good bioactivity, the authors of that research suspected problems of interfacial integrity and strength due to the use of a highly brittle sol-gel glass; similar issues should not apply to the device developed in the present research which is featured by strong materials and interfaces.

4. Conclusions and outlook

This research has demonstrated the feasibility of a novel bioceramic cup coated with a bioactive glass-derived trabecular coating for application in hip joint surgery. The joining between the porous coating and the Al_2O_3/ZrO_2 composite cup was ensured by the interposition of a glass-ceramic interlayer produced by dip-coating technique followed by sintering. From a technological viewpoint, dip-coating method is well understood and simple to perform, relatively inexpensive, quick and versatile. The coating thickness can be tailored by varying the number of dip cycles in a controllable way. By looking at the future scaling-up of the process towards industrial applications, the development of an automatic line system to manipulate the cups would contribute to speed up the manufacturing process as well as to remove any variability introduced by the operator's manual ability; in this regard, critical issues will include the protection of the cup niche that will host the femur head and must remain uncoated, the rotational movement of the cup needed to obtain a coating of homogeneous thickness, and the need for implementing an effective strategy to dry the coating quickly, thus reducing loss of working time.

The research has demonstrated that sponge replication method can be successfully optimized to produce porous products of highly complex shape, such as the hemispherical coating. For this purpose, the research team has designed and developed an effective and versatile set of tools to manipulate the hemispherical sponge/coating over all the phases of the fabrication process, always taking into account the possible scaling-up to an industrial scenario.

This novel acetabular cup allows ceramic-on-ceramic coupling with its well-known anti-wear properties, and the presence of the trabecular glass-derived layer between ceramic cup and host bone can minimize the stiffness mismatch at their interface.

The high mechanical strength of the coatings suggests the suitability of the proposed device under load-bearing conditions, and the good *in vitro* bioactivity of the trabecular layer supports its

osteointegrative potential after implantation. Further mechanical testing on the complete prototype and *in vitro*/*in vivo* biological characterizations, which will deserve to be carried out in a future research, will provide a more comprehensive set of data to support the suitability of this innovative biomedical device.

In summary, the present research is expected to open new perspectives and carries a significant innovation in the field of bioceramic implants for orthopaedic surgery.

Acknowledgements

The research leading to these results has received funding from the EU- FP7/2007-2013 under grant agreement no. 286548 ("Monoblock acetabular cup with trabecular-like coating" – MATCh project).

References

[1] P.F. Gomez, J.A. Morcuende, Early attempts at hip arthroplasty - 1700s to 1950s, Iowa Orthop. J. 25 (2005) 25-29.

[2] A.T. Moore, H.R. Bohlman, Metal hip joint, J. Bone Joint Surg. 25 (1943) 688-692.

[3] D.J. Berry, W.S. Harmsen, M.E. Cabanela, B.F. Morrey, Twenty-five-year survivorship of two thousand consecutive primary Charnley total hip replacements - factors affecting survivorship of acetabular and femoral components, J. Bone Joint Surg. Am. 84 (2002) 171-177.

[4] L.D. Edwards, S. Levin, Complications from total hip replacement with the use of acrylic cement, Health Serv. Rep. 88 (1973) 857-867.

[5] B. Latham, T. Goswami, Effect of geometric parameters in the design of hip implants - paper IV, Mater. Design 25 (2004) 715-722.

[6] A. Sargeant, T. Goswami, Hip implants: Paper V. Physiological effects, Mater. Design 27 (2006) 287-307.

[7] G. Kharmanda, Reliability analysis for cementless hip prosthesis using a new optimized formulation of yield stress against elasticity modulus relationship, Mater. Design 65 (2015) 496-504.

[8] P. Campell, K. DeSmet, Case studies of acetabular loosening in hip resurfacing, in: K. DeSmet, P.N. Campbell, C. Van der Straten (Eds.), The Hip Resurfacing Handbook: A Practical Guide to the Use and Management of Modern Hip Resurfacing, Woodhead Publishing Ltd (Elsevier), Amsterdam, 2013, pp. 454-465.

[9] W.L. Jaffe, D.F. Scott, Current concepts review - total hip arthroplasty with hydroxyapatite-coated prostheses, J. Bone Joint Surg. 78 (1996) 1918-1934.

[10] J.A. D'Antonio, W.N. Capello, W.L. Jaffe, Hydroxylapatite-coated hip implants multicenter three-year clinical and roentgenographic results, Clin. Orthop. Rel. Res. 285 (1992) 102-115.

[11] E. McPherson, L.D. Dorr, T.A. Gruen, M.T. Saberi, Hydroxyapatite-coated proximal ingrowth femoral stems: a matched pair control study, Clin. Orthop. 315 (1995) 223-230.

[12] T. Moilanen, G.W. Stocks, M.A.R. Freeman, G. Scott, W.D. Goodier, S.J.W. Evans, Hydroxyapatite coating of an acetabular prosthesis - effect on stability, J. Bone Joint Surg. 78 (1996) 200-205.

[13] H. McKellop, F.W. Shen, B. Lu, P. Campbell, R. Salovey, Development of an extremely wear-resistant ultra high molecular weight polyethylene for total hip replacements, J. Orthop. Res. 17 (1999) 157-167.

[14] C.H. Geerdink, B. Grimm, R. Ramakrishnan, J. Rondhuis, A.J. Verburg, A.J. Tonino, Crosslinked polyethylene compared to conventional polyethylene in total hip replacement: pre-

clinical evaluation, in vitro testing and prospective clinical follow-up study, Acta Orthop. 77 (2006) 719-725.

[15] M.N. Rahaman, A. Yao, B. Sonny Bal, J.P. Garino, N.D. Ries, Ceramics for prosthetic hip and knee joint replacement, J. Am. Ceram. Soc. 90 (2007) 1965-1988.

[16] A. Buford, T. Goswami, Review of wear mechanisms in hip implants: Paper I – general, Mater. Design 25 (2004) 385-393.

[17] G. Pezzotti, K. Yamamoto, Artificial hip joints: the biomaterials challenge, J. Mech. Behaviour Biomed. Mater. 31 (2014) 3-20.

[18] G. Solarino, A. Abate, A. Morizio, G. Vicenti, B. Moretti, Should we use ceramic-on-ceramic coupling with large head in total hip arthroplasty done for displaced femoral neck fracture?, Semin. Arthroplasty 24 (2013) 255-260.

[19] U. Schreiner, H. Schroeder-Boersch, M. Schwarz, G. Scheller, Improvement of osseointegration of bio-inert ceramics by modification of the surface--results of an animal experiment, Biomed. Tech. (Berl.) 47 (2002) 164-168.

[20] U. Schreiner, A. Schulze, G. Scheller, C. Apruzzese, M.L. Schwarz, Osseointegration of ceramic cement-free acetabular cups, Z. Orthop. Unfall. 150 (2012) 32-39.

[21] E. Verné, C. Vitale-Brovarone, L. Robiglio, F. Baino, Single-piece ceramic prosthesis elements, Patent no. EP2152328 (WO 2008/146322 A2).

[22] L.L. Hench, The story of Bioglass®, J. Mater. Sci. Mater. Med. 17 (2006) 967-978.

[23] L.C. Gerhardt, A.R. Boccaccini, Bioactive glass and glass-ceramic scaffolds for bone tissue engineering, Materials 3 (2010) 3867-3910.

[24] F. Baino, C. Vitale-Brovarone, Three-dimensional glass-derived scaffolds for bone tissue engineering: current trends and forecasts for the future, J. Biomed. Mater. Res. A 97 (2011) 514-535.

[25] Q. Fu, E. Saiz, M.N. Rahaman, A.P. Tomsia, Toward strong and tough glass and ceramic scaffolds for bone repair, Adv. Funct. Mater. 23 (2013) 5461-5476.

[26] C. Vitale-Brovarone, F. Baino, F. Tallia, C. Gervasio, E. Verné, Bioactive glass-derived trabecular coating: a smart solution for enhancing osteointegration of prosthetic elements, J. Mater. Sci. Mater. Med. 23 (2012) 2369-2380.

[27] Q. Chen, F. Baino, N.M. Pugno, C. Vitale-Brovarone, Bonding strength of glass-ceramic trabecular-like coatings to ceramic substrates for prosthetic applications, Mater. Sci. Eng. C 33 (2013) 1530-1538.

[28] F. Baino, F. Tallia, G. Novajra, J. Minguella, M.A. Montealegre, F. Korkusuz, C. Vitale-Brovarone, Novel bone-like porous glass coatings on Al_2O_3 prosthetic substrates, Key Eng, Mater, 631 (2015) 236-240.

[29] F. Baino, C. Vitale-Brovarone, Feasibility of glass-ceramic coatings on alumina prosthetic implants by airbrush spraying method, Ceram. Int. 41 (2015) 2150-2159.

[30] F. Baino, C. Vitale-Brovarone, Trabecular coating on curved alumina substrates using a novel bioactive and strong glass-ceramic, Biomed. Glasses 1 (2015) 31-40.

[31] J. Minguella, D. Cuiñas, J.V. Rodríguez, J. Vivancos, Advanced manufacturing of ceramics for biomedical applications: subjection methods for biocompatible materials, Proc. Eng. 63 (2013) 218-224.

[32] F. Baino, M. Marshall, N. Kirk, C. Vitale-Brovarone ,Design, selection and characterization of novel glasses and glass-ceramics for use in prosthetic applications, Ceram. Int. 42 (2016) 1482-1491.

[33] A.R. Studart, U.T. Gonzenbach, E. Tervoort, L.J. Gauckler, Processing routes to macroporous ceramics: a review, J. Am. Ceram. Soc. 89 (2006) 1771-1789.

[34] F. Baino, C. Vitale-Brovarone, Bioactive glass and glass-ceramic foam scaffolds for bone tissue restoration, in: P.A. Netti (Ed.), Biomedical Foams for Tissue Engineering Applications, Woodhead Publishing Ltd (Elsevier), Amsterdam, 2014, pp. 213-248.

[35] Q. Chen, I.D. Thompson, A.R. Boccaccini, 45S5 Bioglass®-derived glass-ceramic scaffolds for bone tissue engineering, Biomaterials 27 (2006) 2414-2425.

[36] F. Baino, M. Ferraris, O. Bretcanu, E. Verné, C. Vitale-Brovarone, Optimization of composition, structure and mechanical strength of bioactive 3-D glass-ceramic scaffolds for bone substitution, J. Biomater. Appl. 27 (2013) 872-890.

[37] ASTM C633-01, Standard test method for adhesion or cohesion strengthof thermal spray coatings, 2008.

[38] T. Kokubo, H. Takadama, How useful is SBF in predicting in vivo bone bioactivity?, Biomaterials 27 (2006) 2907-2915.

[39] C. Vitale-Brovarone, E. Verné, L. Robiglio, P. Appendino, F. Bassi, G. Martinasso, G. Muzio, R.A. Canuto, Development of glass-ceramic scaffolds for bone tissue engineering: characterisation, proliferation of human osteoblasts and nodule formation, Acta Biomater. 3 (2007) 199-208.

[40] C. Vitale-Brovarone, F. Baino, E. Verné, High strength bioactive glass-ceramic scaffolds for bone regeneration, J. Mater. Sci. Mater. Med. 20 (2009) 643-653.

[41] C. Renghini, V. Komlev, F. Fiori, E. Verné, F. Baino, C. Vitale-Brovarone, Micro-CT studies on 3-D bioactive glass-ceramic scaffolds for bone regeneration, Acta Biomater. 5 (2009) 1328-1337.

[42] C. Renghini, A. Giuliani, S. Mazzoni, F. Brun, E. Larsson, F. Baino, C. Vitale-Brovarone, Microstructural characterization and in vitro bioactivity of porous glass-ceramic scaffolds for bone regeneration by synchrotron radiation X-ray microtomography, J. Eur. Ceram. Soc. 33 (2013) 1553-1565.

[43] R. Polanco, P. Miranzo, M.I. Osendi, Fabrication and microstructure of a ZrO_2-Ni functionally graded bonding interlayer using the airbrush spraying method, Acta Mater. 54 (2006) 2215-2222.

[44] C. Vitale-Brovarone, E. Verné, A. Krajewski, A. Ravaglioli, Graded coatings on ceramic substrates for biomedical applications, J. Eur. Ceram. Soc. 21 (2001) 2855-2862.

[45] F. Baino, C. Vitale-Brovarone, Wollastonite-containing bioceramic coatings on alumina substrates: design considerations and mechanical modelling, Ceram. Int. 41 (2015) 11464-11470.

[46] ISO 13779-4, Implants for Surgery – Hydroxyapatite – Part 4: Determination of Coating Adhesion Strength, 2002.

[47] V. Karageorgiou, D. Kaplan, Porosity of 3D biomaterial scaffolds and osteogenesis, Biomaterials 26 (2005) 5474-5491.

[48] L.L. Hench, Bioceramics: from concept to clinic, J. Am. Ceram. Soc. 74 (1991) 1487-1510.

[49] L.L. Hench, Bioactive ceramics, Ann. N.Y. Acad. Sci. 523 (1988) 54-57.

[50] M. Hamadouche, A. Meunier, D.C. Greenspan, C. Blanchat, J.P. Zhong, G.P. La Torre, L. Sedel, Bioactivity of sol-gel bioactive glass coated alumina implants, J. Biomed. Mater. Res. 52 (2000) 422-429.

Figure captions

Figure 1. The concept behind the research work reported in this article: the novel acetabular cup for hip joint prosthesis disclosed in the patent [21] and developed by the authors in the framework of the EC-funded project "MATCh".

Figure 2. Preparation of the S57A7 coating (interlayer): (a,b) dipping of the bioceramic cup into the S57A7 slurry, (c) cup extraction from the slurry and (d) removal of the glass-coated cup from the sample-holder.

Figure 3. Shaping of the polymer sponge used as a template for the shell-like trabecular coating: (a) assembling of the metal mould with placement of the sponge sheet, (b) opening of the mould and extraction of the shaped sponge (hemispherical shell), (c) cross-section of the shaped sponge, (d) hemispherical sponge attached to the bioceramic cup (ready to be processed by the sponge replica method).

Figure 4. Novel application of the sponge replica method to produce the hemispherical trabecular coating. The macrophotograph (inset) illustrates the components of the sample-holder and squeezing system for the cup: 1 = perforated plastic hemi-shells, 2 = supporting plate, 3 = hollow peg (already shown in Fig. 2), 4 = supporting cylinder to be connected to the plate. The two drawings on the top illustrate the action of the squeezing devices (perforated hemi-shells) on the horizontal plane: configurations at the end of the phase of pressing along the direction y (left) and at the end of the subsequent phase of pressing along the direction x (right). The three drawings on the bottom illustrate the action of the squeezing devices (perforated hemi-shells) on the vertical plane: starting configuration (left), vertical pressing along the direction y (centre), horizontal pressing

along the direction x (right). There is a direct correspondence (compressions on the horizontal and vertical planes) between the drawings in the central and right position.

Figure 5. Visualization of the key phases of the foam replica method applied innovatively to the hemispherical sponge: (a) positioning of the sample (cup coated with the slurry-impregnated sponge), anchored to the sample holder, on the supporting plate, (b) squeezing by horizontal and vertical compression (details shown in Fig. 4), (c,d) complete "green" samples (ready to be thermally treated for sintering).

Figure 6. S57A7 coating: (a) "green" sample (glass-coated cup prior to sintering), (b, c) sintered coatings on small and large bioceramic cups.

Figure 7. Morphological investigation of the S57A7 coating: SEM cross-sectional images acquired at low (50×) (a) and high magnification (1600×) (b); micro-tomographic reconstruction of the 3-D whole volume (c) and cross-sectional image with emphasized contrast (d).

Figure 8. Elemental line profiles (EDS analysis) for O, Na, Al, Si, Zr and Ca in the bioceramic cup/S57A7 coating interfacial area. SEM picture magnification is 1700×.

Figure 9. Complete sample after sintering: (a) upward and (b) downward perspective views; (c) 3-D tomographic reconstruction of the trabecular coating (visualized as "separated" from the substrate) and (d) SEM micrographs that shows the typical bone-like architecture of the trabecular layer with its interconnected pores and struts (magnification 300×).

Figure 10. Micro-tomographic investigations: (a) X-ray shadow image of the sample (the trabecular coating attached to the cup is clearly evident), (b-f) cross-sections of the sample parallel to the cup

axis through the top of the cup, (860 µm distance between cross-sections), (g) 3-D visualization of the structure of the trabecular layer.

Figure 11. *In vitro* bioactivity test: (a) SEM cross-sectional image of a complete sample after soaking for 7 days in SBF (magnification 180×) and (b) detail of the newly formed CaP layer formed on the struts (magnification 2000×) with the corresponding compositional analysis (EDS).

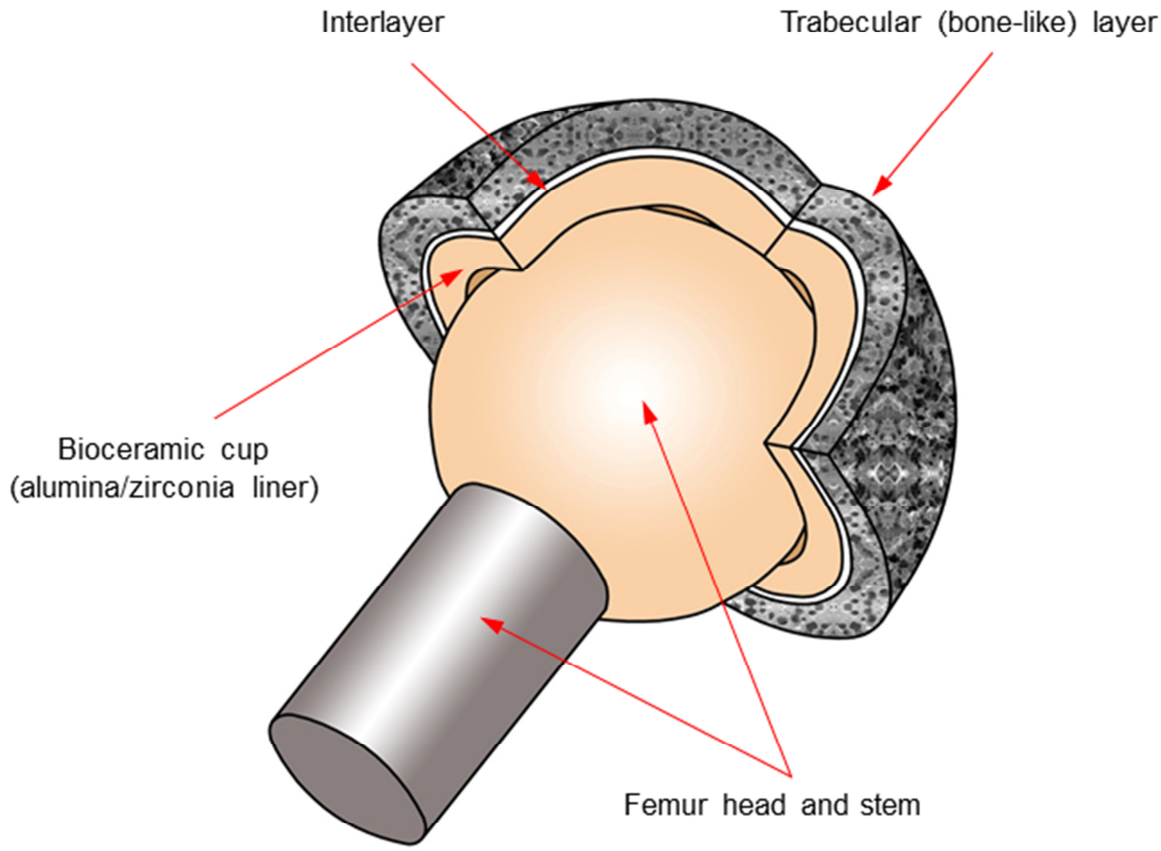
Interlayer
Trabecular (bone-like) layer
Bioceramic cup
(alumina/zirconia liner)
Femur head and stem

Fig. 1

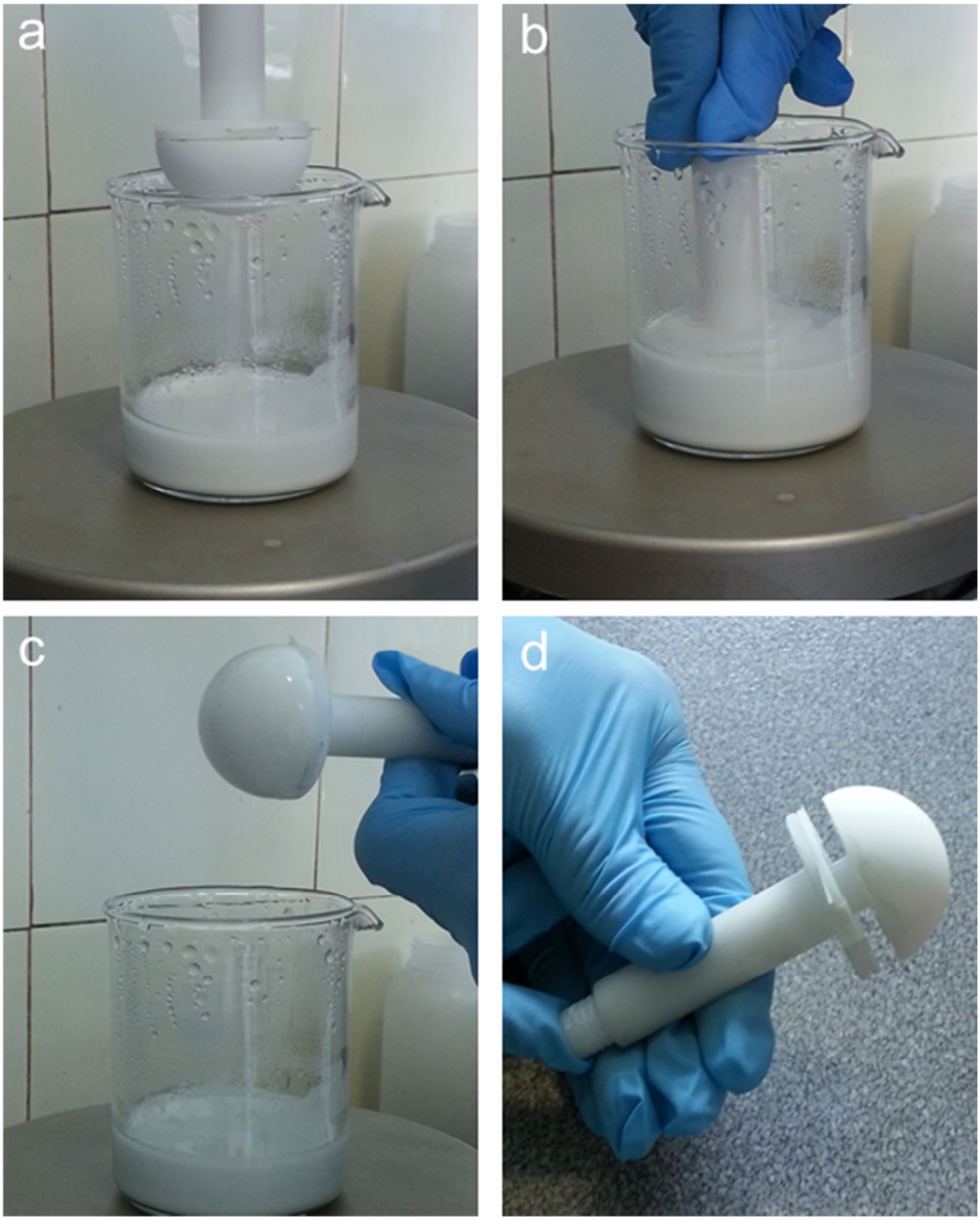

Fig. 2

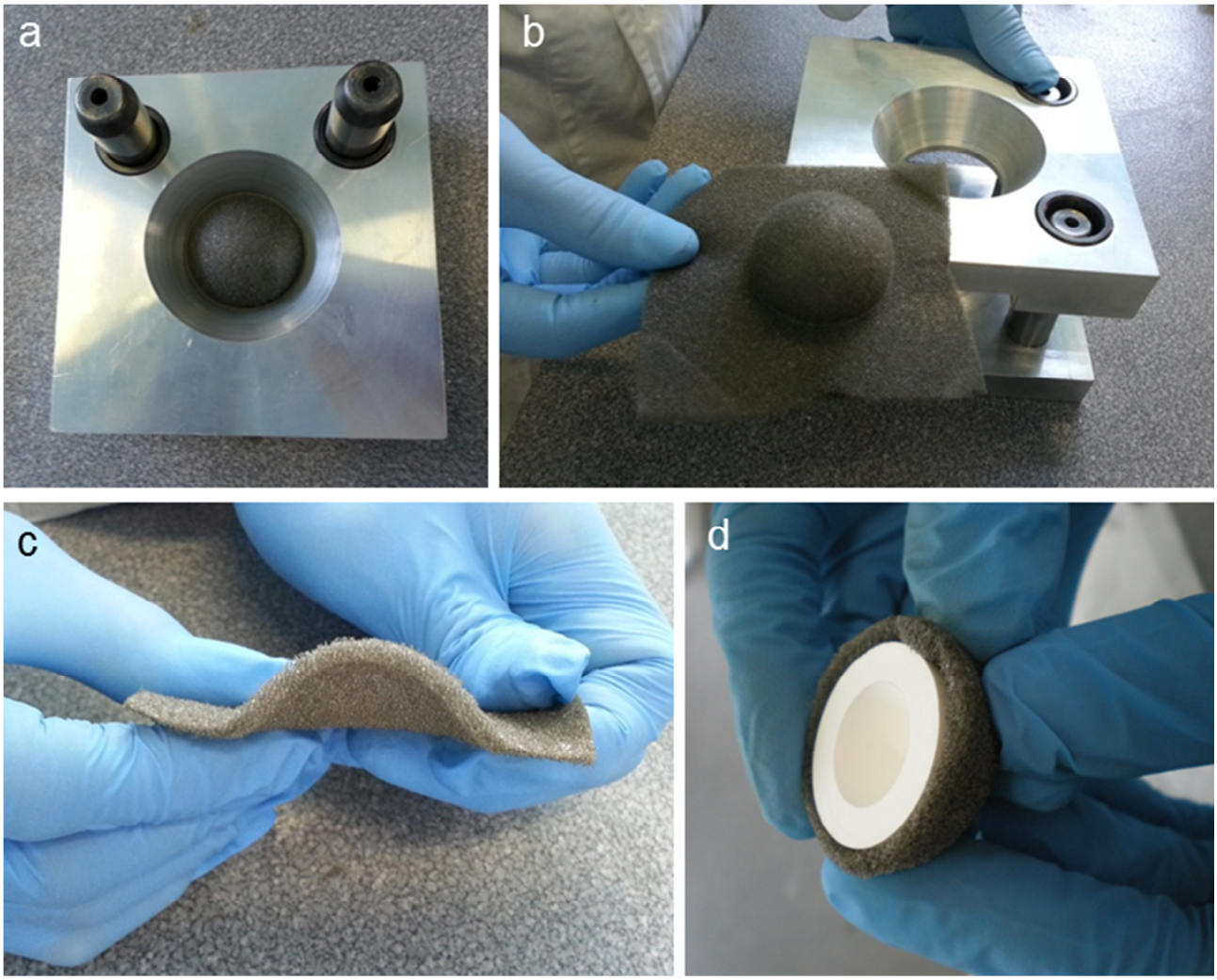

Fig. 3

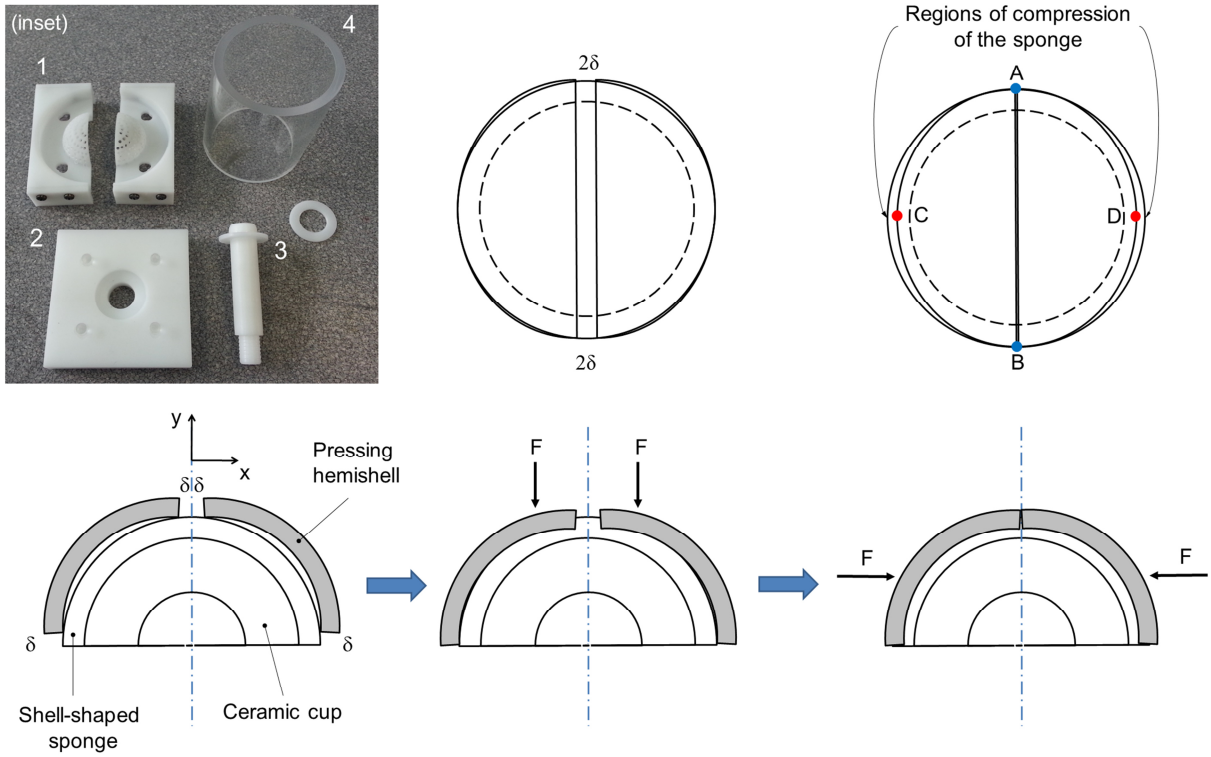
(inset)
1
2
3
4
2δ
2δ
Regions of compression
of the sponge
A
B
C
D
y
x
δ δ
Pressing
hemishell
δ
δ
Shell-shaped
sponge
Ceramic cup
F
F
F
F

Fig. 4

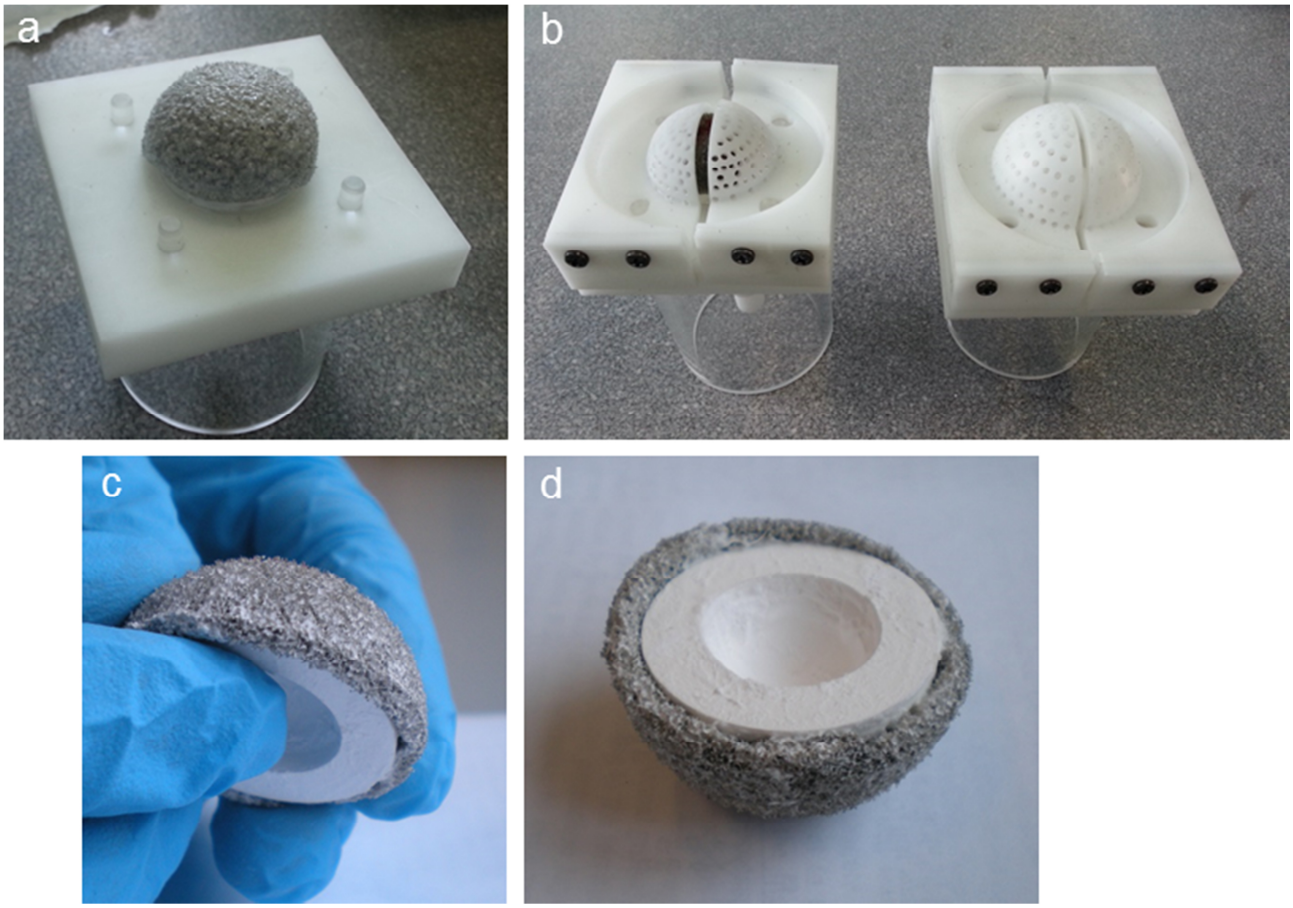

Fig. 5

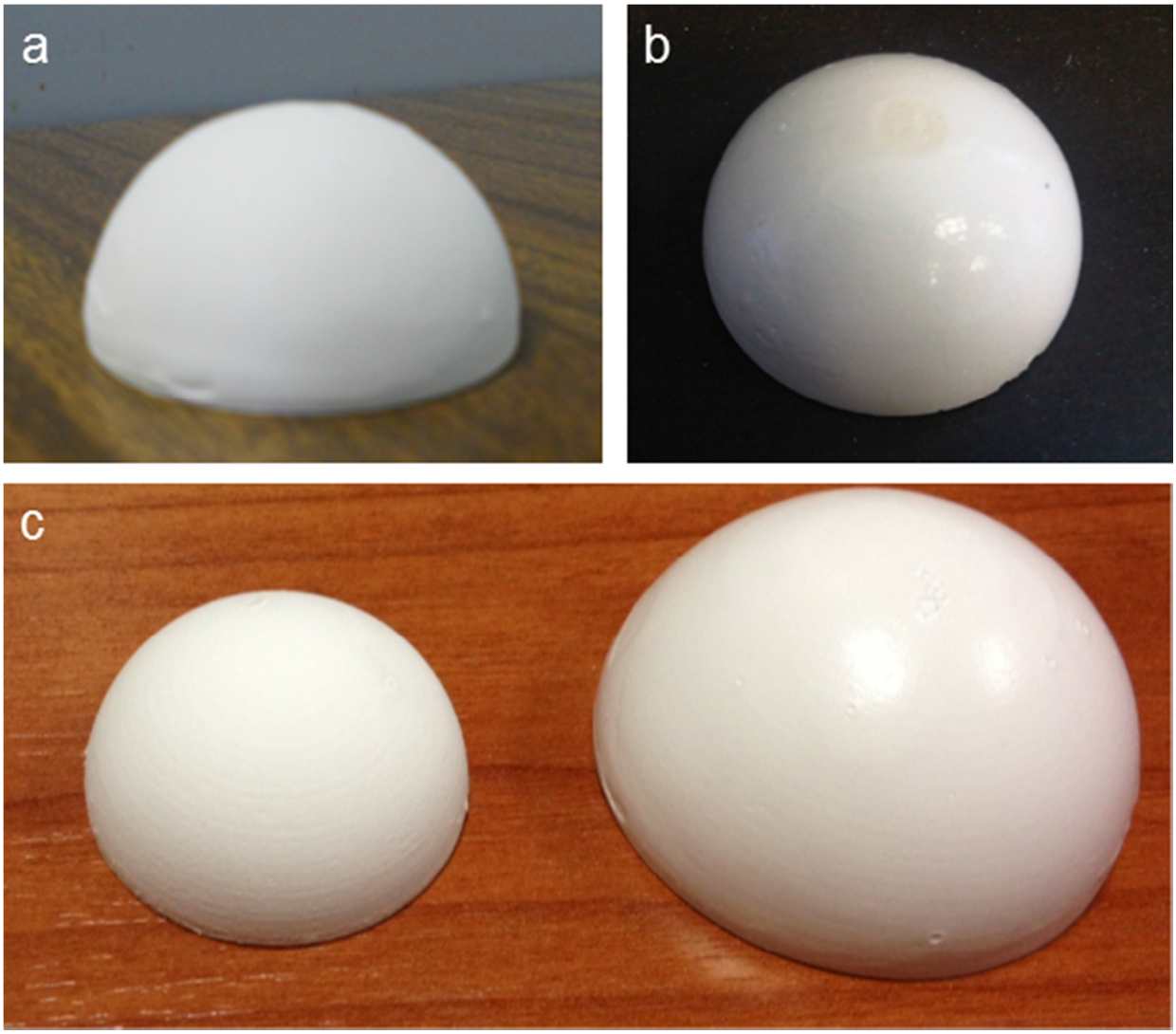

Fig. 6

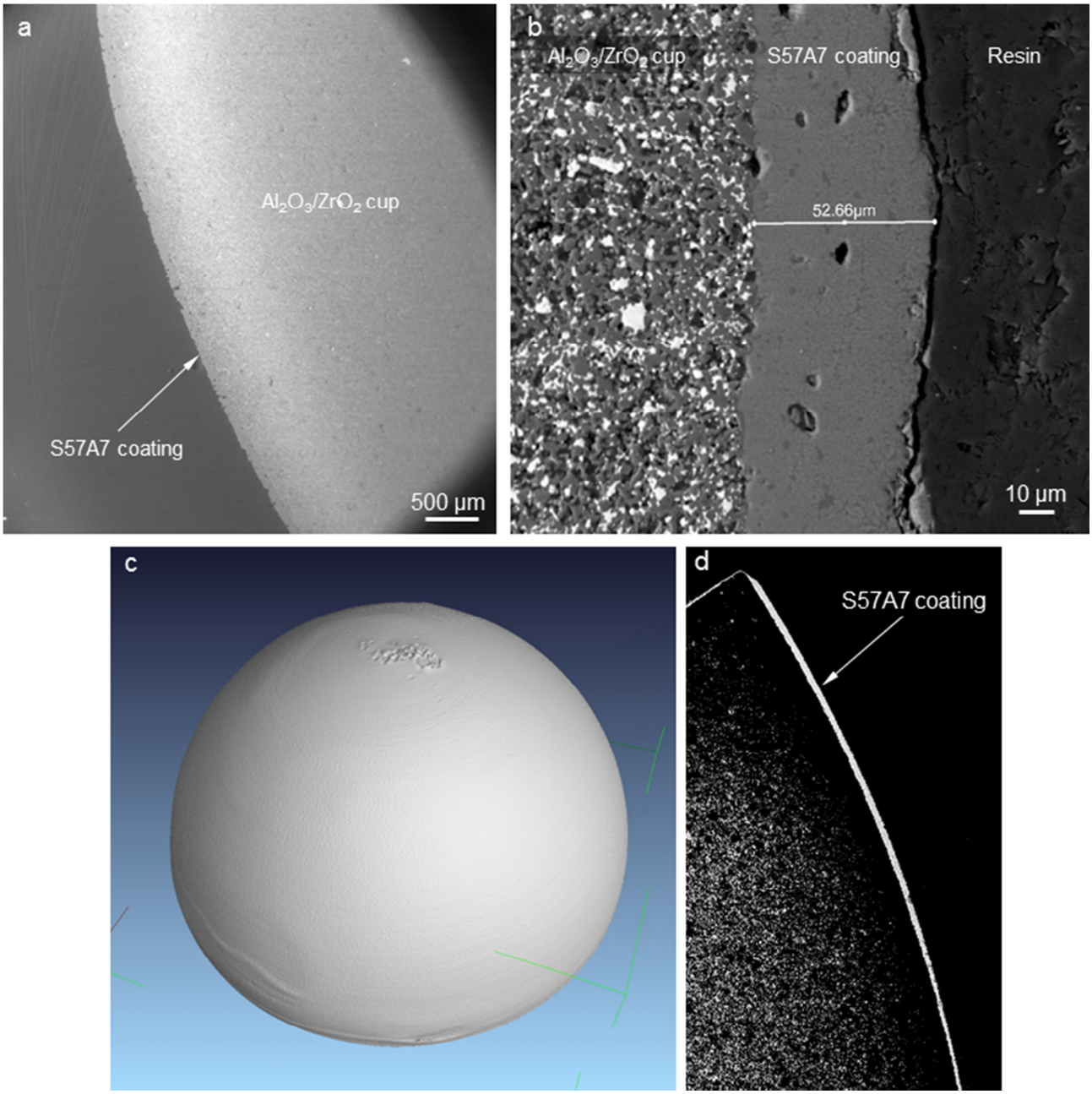
a
Al_2O_3/ZrO_2 cup
S57A7 coating
500 μm
b
Al_2O_3/ZrO_2 cup
S57A7 coating
Resin
52.66μm
10 μm
c
d
S57A7 coating

Fig. 7

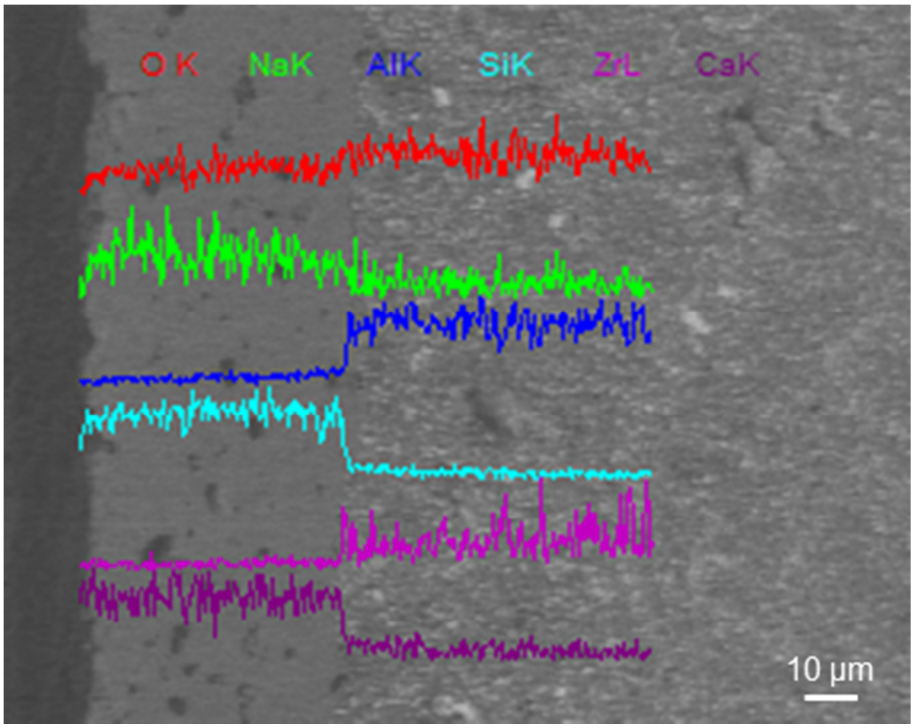

Fig. 8

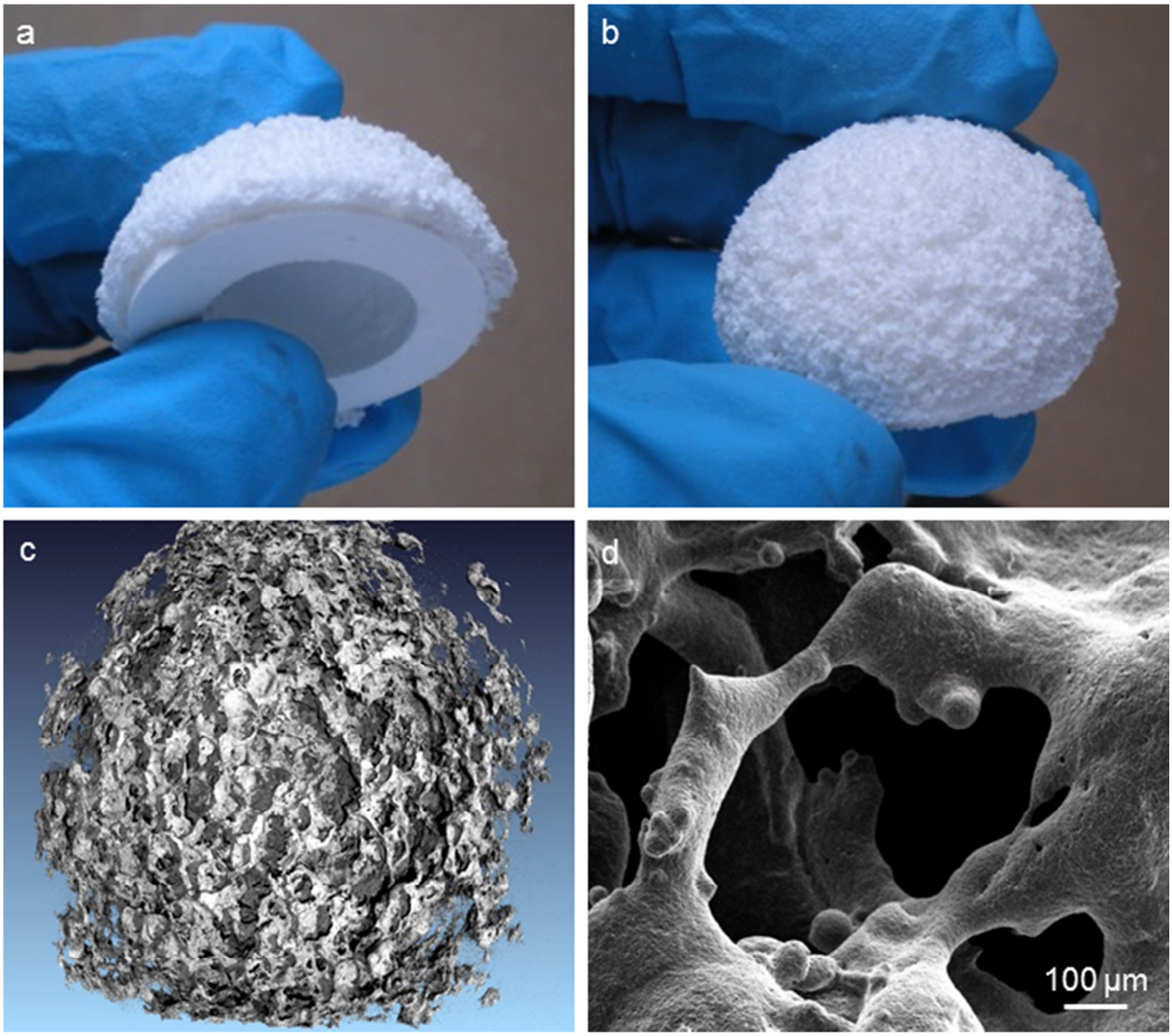

Fig. 9

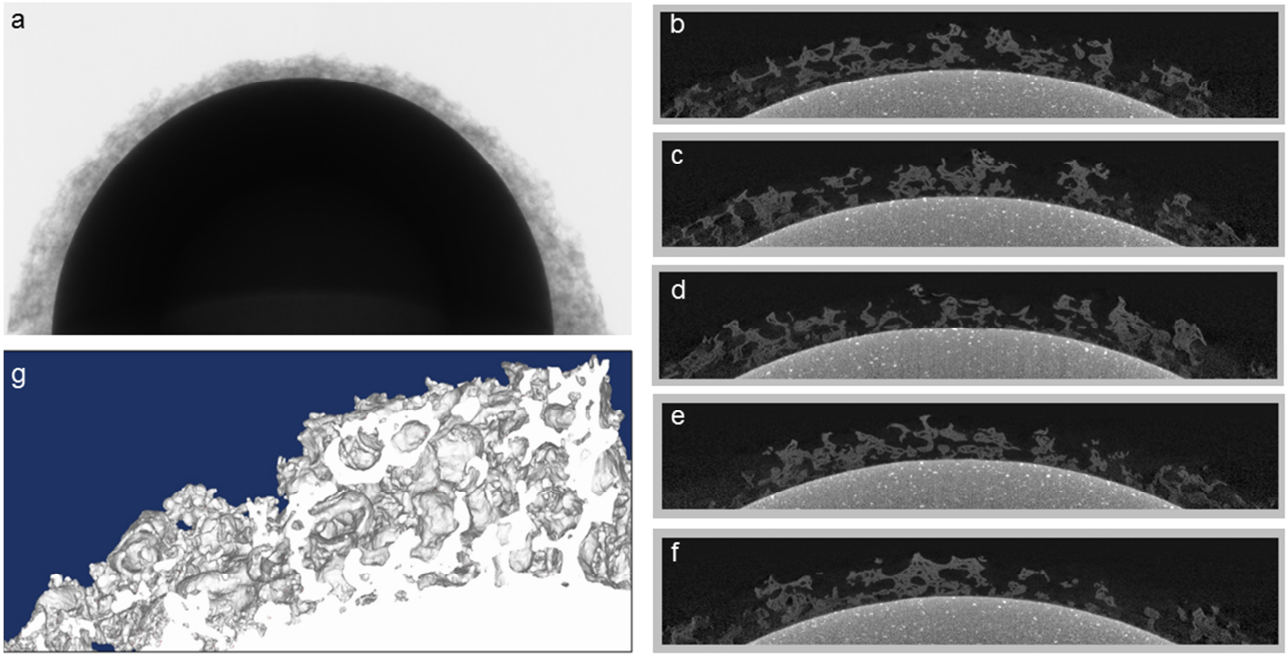

Fig. 10

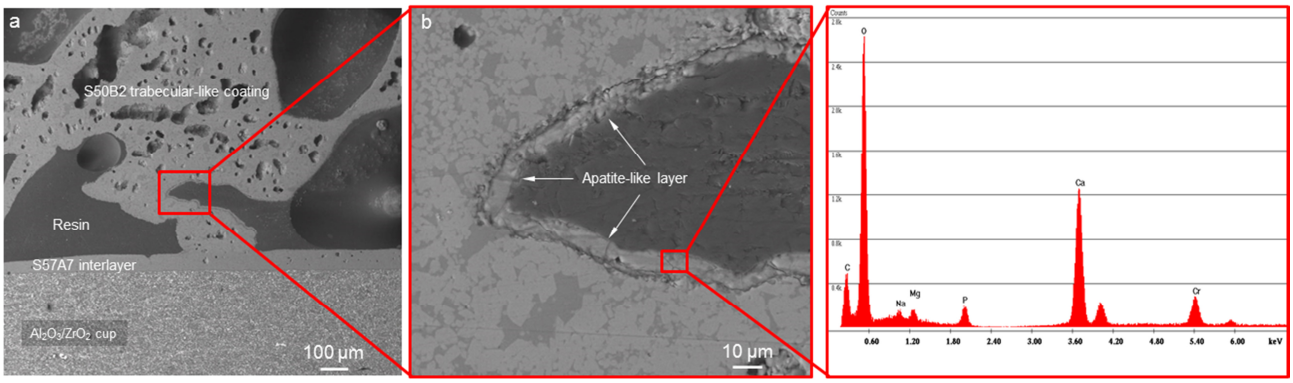
a
S50B2 trabecular-like coating
Resin
S57A7 interlayer
Al_2O_3/ZrO_2 cup
100 μm
b
Apatite-like layer
10 μm
O
Ca
C
Mg
Na
P
Cr
0.60
1.20
1.80
2.40
3.00
3.60
4.20
4.80
5.40
6.00
keV

Fig. 11